

The 2-Pyroxene Geothermometer of the Kapalagulu Layered Intrusion, Tanzania, East Africa

Ahmed A. Almohandis

Geology Department, College of Science, University of Riyadh, Riyadh, Saudi Arabia.

The kapalagulu intrusion in Western Tanzania is a layered sequence of ultrabasic and basic cumulates. It consists of olivine, plagioclase, Ca-poor and Ca-rich pyroxenes as the major minerals.

The 2-pyroxene geothermometry of Wood and Banno was applied to investigate the cooling stages in the intrusion compared with the remarkable cryptic variation displayed by Ca-poor Pyroxene.

The Ca-poor pyroxene shows a phase change from primary orthopyroxene to inverted pigeonite at a lower temperature ($< 1000^{\circ}\text{C}$) than that of the Bushveld at similar compositional range, for both intrusions.

The equilibration temperatures for exsolution lamellae in the inverted pigeonite was also determined.

The Kapalagulu intrusion is a layered sequence of ultrabasic and basic cumulates. It occurs as a long, tabular body approximately 14.5 km by 1.6 km. It is located some 112 km, South of Kigoma town, Western Tanzania, East Africa. A geological map of the intrusion with sample locations is shown in Fig. 1.

The intrusion consists of three major Zones; the Basal, Intermediate and Main Zone. The Main Zone has been divided into five sub-zones; namely, MZa, MZb, MZc, MZd and MZe (Wadsworth 1963, Almohandis 1977).

The cumulus mineralogy of the Kapalagulu intrusion is simple with olivine, plagioclase, Ca-poor and Ca-rich Pyroxenes as the major minerals. Minor cumulus chromite occurs only in the Basal Zone, usually with immiscible sulphides and biotite. Cumulus ilmenite and apatite occur only in the upper layered series of the Main Zone. The cumulus mineralogy, phase layering, mineral compositions, and the

nomenclature of the Kapalagulu Zones and Sub zones are summarized in Fig. 2 using an arbitrary height scale.

The purpose of this paper is to apply the 2-Pyroxene geothermometer (OPX-CPX) on the Kapalagulu layered series and to investigate the cooling history compared with the distinctive cryptic variation displayed by the mineral compositions, especially Ca-poor-Pyroxene.

Potential Geothermometers

There are many potential geothermometers in which the effect of pressure can be ignored (Carmichael *et al.*, 1974) Some of these geothermometers have been calibrated experimentally. The principle of estimating the geothermometry in petrology depends on the thermodynamic calculations. Thus, Carmichael *et al.* (1974) showed that $(\partial \Delta G_{T^{\circ}} / \partial P) = \Delta V^{\circ} \simeq 0$, which indicates that ΔV° is the sum of the molar volumes of the products less that of the reactants, all in their standard states at constant temperature.

The most useful geothermometers at the present time include the Ni geothermometer of Hakli and Wright (1967), the apatite-phlogopite geothermometer (Ludington 1973), the iron-titanium oxide geothermometer (Buddington and Lindsley 1964), the pyrrhotite-pyrite geothermometer (Toulmin and Barton 1964), and the orthopyroxene-clinopyroxene geothermometer (OPX-CPX) (Boyd 1969).

The OPX-CPX geothermometer

This geothermometer is based on the fact that Ca-rich pyroxene and Ca-poor pyroxene are immiscible over a wide range of temperature and composition. Davis and Boyd (1966) found that the immiscibility region for the magnesian end member is relatively unaffected by pressure. They found that the solubility of enstatite in Ca-rich pyroxene is temperature dependent.

Methods of estimating the equilibration temperatures of coexisting pyroxenes in the system $\text{CaSiO}_3 - \text{MgSiO}_3 - \text{FeSiO}_3$ have been advanced by Wood and Banno (1973), Saxena and Nehru (1975) and Ross and Huebner (1975). The first method of Wood and Banno was determined to be the most appropriate and accurate method in the present study. This method enables equilibration temperatures of coexisting pyroxenes to be calculated with a reasonable degree of accuracy which should produce results accurate to about 70°C (Wood and Banno 1973).

All the equilibration temperatures of the available coexisting pyroxenes have been calculated using the following equation:

$$T = \frac{-10202}{2.303 \log_{10} \left(\frac{\text{CPX}_a \text{Mg}_2\text{Si}_2 \text{O}_6}{\text{OPX}_a \text{Mg}_2\text{Si}_2 \text{O}_6} \right) - 7.65 X_{\text{Fe}}^{\text{OPX}} + 3.88 (X_{\text{Fe}}^{\text{OPX}})^2 - 4.6}$$

T is the temperature of equilibration in K °

$\text{PyX}_a \text{Mg}_2 \text{Si}_2 \text{O}_6$ is the activity of enstatite in Ca-rich pyroxene which equals:

$$Y(M1) \cdot Y(M2) \cdot \left(\frac{\text{Mg}}{\text{Mg} + \text{Fe}} \right)^2 \text{PyX}.$$

Y (M1) and Y (M2) are M1 and M2 sites that remain after subtracting the occupancies of these sites by the octahedrally coordinated ions assuming that the large ions such as Ca^{2+} and Mn^{2+} present in the ortho and clinopyroxene structure occupy M2 while the smaller octahedrally coordinated ions such as Al^{3+} , Cr^{3+} and Ti^{4+} occupy M1 site.

$$X_{\text{Fe}}^{\text{OPX}} = \frac{(\text{Fe}^{2+})}{\text{Fe}^{2+} + \text{Mg}^{2+}}$$

The equilibration temperatures of Ca-rich and Ca-poor pyroxene pairs are shown in Table 1, while the equilibration temperatures of subsolidus lamellae are shown in Table 2.

Method of Pyroxene Analysis

Analysis of pyroxene was carried out using a Cambridge Geoscan II electron microanalyser. An accelerating voltage of 15 KV and a specimen current of 1.8×10^{-8} amps. was used. A beam focussed to a diameter of approximately 2-3 microns was maintained. Standards used were synthetic and natural minerals and pure metals. Data processing was by the computer program of Rucklidge and Gaspirini (1969).

Discussion

The equilibration temperatures and the MgR ($100 \text{ Mg}/\text{Mg}^{2+} + \text{Fe}^{2+} + \text{Mn}^{2+}$) of Ca-poor pyroxene have been plotted in Fig. 3 to show the equilibration temperatures and the cryptic variation along the stratigraphic succession of the Kapalagulu layered Series. Although the variation of equilibration temperatures should reflect generally the iron-enrichment in Ca-poor pyroxene, they failed to show continuous and consistent relationships with the changing composition of pyroxene. This is due probably to the fact that Ca-rich pyroxene occurs as an intercumulus phase in some samples, and to the uncertainties in the method ($\pm 70^\circ$, Wood and Banno 1973). However, the marked reversals in cryptic variation shown by Ca-poor pyroxene at the bottom of MZd are also indicated in the equilibration temperatures diagram (Almohandis 1977).

The Ca-poor pyroxene of the Kapalagulu intrusion shows a phase change from primary orthopyroxene to inverted pigeonite at a composition (on Ca-free basis) between $\text{Mg}_{70} \text{Fe}_{30}$ and $\text{Mg}_{60} \text{Fe}_{40}$ which is almost similar to the compositional range

established for the phase change in the Bushveld intrusion (Atkins 1969). However, the point where primary orthopyroxene ceases to form and inverted pigeonite begins to crystallize, is at a lower temperature for the Kapalagulu magma (< 1000 °C) than that of the Bushveld magma (1005 °C, Wood and Banno 1973). The Kapalagulu and Skaergaard pyroxenes would have almost similar miscibility gaps and the orthopyroxene-inverted pigeonite changeover takes place at $Mg_{70}Fe_{30}$ in both intrusions. Thus, it is suggested that the difference in the crystallization temperature of pyroxenes of comparable composition from the two intrusions is small. Consequently, the pressure of crystallization of the Kapalagulu intrusion is probably similar or comparable with the 600 bars given for Skaergaard (Lindsley *et al.* 1969).

The equilibration temperature for subsolidus lamellae in the inverted Pigeonite of the MZc (Subzone C of the Main Zone) is 919 °C, while it is between 846 °C and 752 °C for the inverted pigeonite of the MZe (Subzone E of the Main Zone). This is probably the result of slightly higher temperature of formation of the subsolidus lamellae of MZc with slow diffusion of Ca and subsequently their coarser nature and their crystallization under equilibrium conditions. The exsolution lamellae in the inverted pigeonite of MZe is much finer than those of the MZc.

Acknowledgement: I should like to thank Dr. A.C. Dunham for helpful discussions and constant encouragement, Dr. W.J. Wardsworth for providing samples, air photos with continuous encouragement, and to Prof. A.S. Rogers for reviewing the manuscript.

References

- Almohandis, A.A. (1977) Mineralogy of the Kapalagulu layered intrusion. Tanzania. *Ph.D Thesis*, University of Manchester. U.K. (*Unpublished*).
- Atkins, F.B. (1969) Pyroxenes of the Bushveld intrusion, South Africa, *J. Petrol.*, **10**, 222-249.
- Boyd, F.R. (1969) Electron-Probe study of diopside inclusions from Kimberlite, *Am. J. Sci.*, **267 A**, 50-69.
- Buddington, A.F. and Lindsley, D.H. (1964) Iron-titanium oxide minerals and Synthetic equivalents. *J. Petrol.*, **5**, 310-357.
- Carmichael, I.S.E., Turner, F.J. and Verhoogen, J. (1974) *Igneous Petrology*, 739 McGraw-Hill : New York.
- Davis, B.T.C. and Boyd, F.R. (1966) The join $Mg_2Si_2O_6 - CaMgSi_2O_6$ at 30 Kilobars Pressure and its application to Pyroxenes from Kimberlites. *J. Geophys. Res.*, **71**, 3567-76.
- Hakli, T.A. and Wright, T.L. (1967) The fractionation of nickel between olivine and augite as a geothermometer. *Geochim. Cosmochim. Acta*, **31**, 877-884.
- Lindsley, D.H., Brown, G.M. and Muir, I.D. (1969) Conditions of the ferrowollastonite - ferrohedenbergite inversion in the Skaergaard intrusion: East Greenland. In: J.J. Papike (Ed.), Pyroxenes and amphiboles: Crystal chemistry and Phase Petrology. *Min. Soc. Am. Spec. Paper*, No. 2, 193-201.
- Ludington, S.D. (1973) Refinement of the biotite-apatite geothermometer. *Geol. Soc. Am. Abstracts*, **5**, 493-494.
- Ross, M. and Huebner, S. (1975) Estimation of the minimum temperature for coexistence of orthopyroxene, Pigeonite and augite and its application to prediction of temperature of crystallization of lunar pyroxenes. *Proceeding of the 6th Lunar Science Conf.* 689-91.

- Rucklidge and Gasparini** (1969) *Specification of a Computer Program for Processing Microprobe Data*, EMPADR VII. Publ. of Geol. Dept. of Toronto Univ., Ontario, Canada.
- Saxena, S.K. and Nehru, C.E.** (1975) Enstatite-Diopside solvus and geothermometry. *Contr. Mineral. Petrol.*, **49**, 259-267.
- Toulmin, P. and Barton, P.B.** (1964) A thermodynamic study of pyrite and pyrrhotite. *Geochim. Cosmochim. Acta*, **28**, 641-671.
- Wadsworth, W.J.** (1963) The Kapalagulu layered intrusion of Western Tanganyika. *Min. Soc. Amer. Special Paper 1*, 108-15.
- Wood, B.J. and Banno, S.** (1973) Garnet - orthopyroxene and orthopyroxene-clinopyroxene relationships in simple and complex systems. *Contr. Mineral. Petrol.*, **42**, 109-24.

Table 1. Equilibration Temperatures

Pyroxene Pair		Y(M1)	Y(M2)	PYX_a Mg ₂ Si ₂ O ₆	Fe/Fe + Mg	Mg/Mg + Fe	T ° K	T ° C
Basal Zone								
K250	Opx *	0.93	0.939	0.635	0.148	0.852	1321.3	1048.3
	Cpx *	0.878	0.119	0.798	0.126	0.874		
Intermediate Zone								
K237	Opx	0.924	0.939	0.602	0.167	0.833	1404.3	1131.3
	Cpx *	0.891	0.215	0.132	0.160	0.840		
K26	Opx	0.932	0.897	0.540	0.196	0.804	1225.6	952.6
	Cpx	0.869	0.080	0.050	0.149	0.851		
Main Zone								
K30	Opx	0.946	0.934	0.618	0.164	0.836	1262.3	989.3
	Cpx *	0.888	0.090	0.060	0.135	0.865		
K31	Opx	0.942	0.924	0.614	0.160	0.840	1372.1	1099.1
	Cpx *	0.874	0.167	0.111	0.128	0.872		
K334	Opx	0.942	0.931	0.527	0.225	0.775	1234.5	961.5
	Cpx	0.894	0.107	0.062	0.195	0.805		

Table 1. Equilibration Temperatures (CONTD)

Pyroxene Pair		Y(M1)	Y(M2)	$PYX_{aMg_2Si_2O_6}$	Fe/Fe + Mg	Mg/Mg + Fe	T° K	T° C																																																																																																						
K34	Opx	0.932	0.992	0.564	0.219	0.781	1211.0	938.0																																																																																																						
	Cpx	0.893	0.094	0.055	0.188	0.812			K128	Opx	0.950	0.917	0.457	0.276	0.724	1158.7	885.7	Cpx*	0.908	0.076	0.042	0.218	0.782	K337	Opx	0.960	0.918	0.374	0.349	0.651	1218.9	945.9	Cpx	0.903	0.161	0.078	0.269	0.731	K61	Opx	0.951	0.943	0.514	0.243	0.757	1268.7	995.7	Cpx*	0.874	0.161	0.084	0.227	0.773	K62	Opx	0.953	0.924	0.558	0.204	0.796	1276.6	1003.6	Cpx	0.926	0.117	0.076	0.162	0.838	K63	Opx	0.966	0.845	0.471	0.240	0.760	1242.9	969.9	Cpx	0.940	0.102	0.064	0.182	0.818	K65	Opx	0.958	0.938	0.537	0.227	0.773	1229.0	956.0	Cpx*	0.939	0.098	0.064	0.169	0.831	K65a	Opx	0.958	0.865	0.418	0.290	0.710	1320.9	1047.9	Cpx*	0.899	0.234
K128	Opx	0.950	0.917	0.457	0.276	0.724	1158.7	885.7																																																																																																						
	Cpx*	0.908	0.076	0.042	0.218	0.782			K337	Opx	0.960	0.918	0.374	0.349	0.651	1218.9	945.9	Cpx	0.903	0.161	0.078	0.269	0.731	K61	Opx	0.951	0.943	0.514	0.243	0.757	1268.7	995.7	Cpx*	0.874	0.161	0.084	0.227	0.773	K62	Opx	0.953	0.924	0.558	0.204	0.796	1276.6	1003.6	Cpx	0.926	0.117	0.076	0.162	0.838	K63	Opx	0.966	0.845	0.471	0.240	0.760	1242.9	969.9	Cpx	0.940	0.102	0.064	0.182	0.818	K65	Opx	0.958	0.938	0.537	0.227	0.773	1229.0	956.0	Cpx*	0.939	0.098	0.064	0.169	0.831	K65a	Opx	0.958	0.865	0.418	0.290	0.710	1320.9	1047.9	Cpx*	0.899	0.234	0.122	0.238	0.762												
K337	Opx	0.960	0.918	0.374	0.349	0.651	1218.9	945.9																																																																																																						
	Cpx	0.903	0.161	0.078	0.269	0.731			K61	Opx	0.951	0.943	0.514	0.243	0.757	1268.7	995.7	Cpx*	0.874	0.161	0.084	0.227	0.773	K62	Opx	0.953	0.924	0.558	0.204	0.796	1276.6	1003.6	Cpx	0.926	0.117	0.076	0.162	0.838	K63	Opx	0.966	0.845	0.471	0.240	0.760	1242.9	969.9	Cpx	0.940	0.102	0.064	0.182	0.818	K65	Opx	0.958	0.938	0.537	0.227	0.773	1229.0	956.0	Cpx*	0.939	0.098	0.064	0.169	0.831	K65a	Opx	0.958	0.865	0.418	0.290	0.710	1320.9	1047.9	Cpx*	0.899	0.234	0.122	0.238	0.762																											
K61	Opx	0.951	0.943	0.514	0.243	0.757	1268.7	995.7																																																																																																						
	Cpx*	0.874	0.161	0.084	0.227	0.773			K62	Opx	0.953	0.924	0.558	0.204	0.796	1276.6	1003.6	Cpx	0.926	0.117	0.076	0.162	0.838	K63	Opx	0.966	0.845	0.471	0.240	0.760	1242.9	969.9	Cpx	0.940	0.102	0.064	0.182	0.818	K65	Opx	0.958	0.938	0.537	0.227	0.773	1229.0	956.0	Cpx*	0.939	0.098	0.064	0.169	0.831	K65a	Opx	0.958	0.865	0.418	0.290	0.710	1320.9	1047.9	Cpx*	0.899	0.234	0.122	0.238	0.762																																										
K62	Opx	0.953	0.924	0.558	0.204	0.796	1276.6	1003.6																																																																																																						
	Cpx	0.926	0.117	0.076	0.162	0.838			K63	Opx	0.966	0.845	0.471	0.240	0.760	1242.9	969.9	Cpx	0.940	0.102	0.064	0.182	0.818	K65	Opx	0.958	0.938	0.537	0.227	0.773	1229.0	956.0	Cpx*	0.939	0.098	0.064	0.169	0.831	K65a	Opx	0.958	0.865	0.418	0.290	0.710	1320.9	1047.9	Cpx*	0.899	0.234	0.122	0.238	0.762																																																									
K63	Opx	0.966	0.845	0.471	0.240	0.760	1242.9	969.9																																																																																																						
	Cpx	0.940	0.102	0.064	0.182	0.818			K65	Opx	0.958	0.938	0.537	0.227	0.773	1229.0	956.0	Cpx*	0.939	0.098	0.064	0.169	0.831	K65a	Opx	0.958	0.865	0.418	0.290	0.710	1320.9	1047.9	Cpx*	0.899	0.234	0.122	0.238	0.762																																																																								
K65	Opx	0.958	0.938	0.537	0.227	0.773	1229.0	956.0																																																																																																						
	Cpx*	0.939	0.098	0.064	0.169	0.831			K65a	Opx	0.958	0.865	0.418	0.290	0.710	1320.9	1047.9	Cpx*	0.899	0.234	0.122	0.238	0.762																																																																																							
K65a	Opx	0.958	0.865	0.418	0.290	0.710	1320.9	1047.9																																																																																																						
	Cpx*	0.899	0.234	0.122	0.238	0.762																																																																																																								

Table 1. Equilibration Temperatures (contd.)

Pyroxene Pair		Y(M1)	Y(M2)	PYX _a Mg ₂ Si ₂ O ₆	Fe/Fe + Mg	Mg/Mg + Fe	T ° K	T ° C
Main Zone (contd.)								
K66	Opx	0.959	0.917	0.452	0.283	0.717	1252.9	979.9
	Cpx*	0.909	0.167	0.088	0.240	0.760		
K172	Opx	0.959	0.915	0.405	0.321	0.679	1224.9	951.9
	Cpx*	0.886	0.174	0.076	0.297	0.709		
K67	Opx	0.959	0.910	0.395	0.327	0.673	1216.1	943.1
	Cpx	0.912	0.141	0.072	0.251	0.749		
K68	Opx	0.958	0.890	0.350	0.359	0.641	1212.5	939.5
	Cpx	0.914	0.162	0.073	0.300	0.700		
K69	Opx	0.949	0.918	0.321	0.393	0.607	1203.8	930.8
	Cpx	0.899	0.180	0.074	0.325	0.675		
K70	Opx	0.946	0.907	0.311	0.398	0.602	1197.2	924.2
	Cpx	0.920	0.183	0.070	0.357	0.643		
K263	Opx	0.957	0.814	0.199	0.494	0.506	1213.4	940.4
	Cpx	0.910	0.227	0.075	0.400	0.601		

* indicates intercumulus

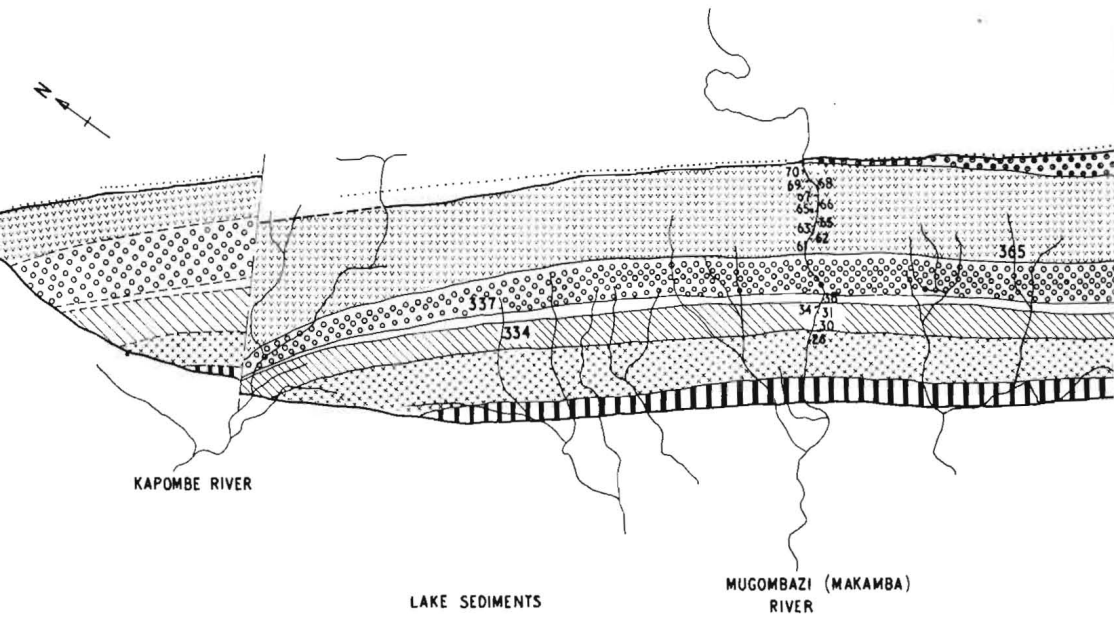
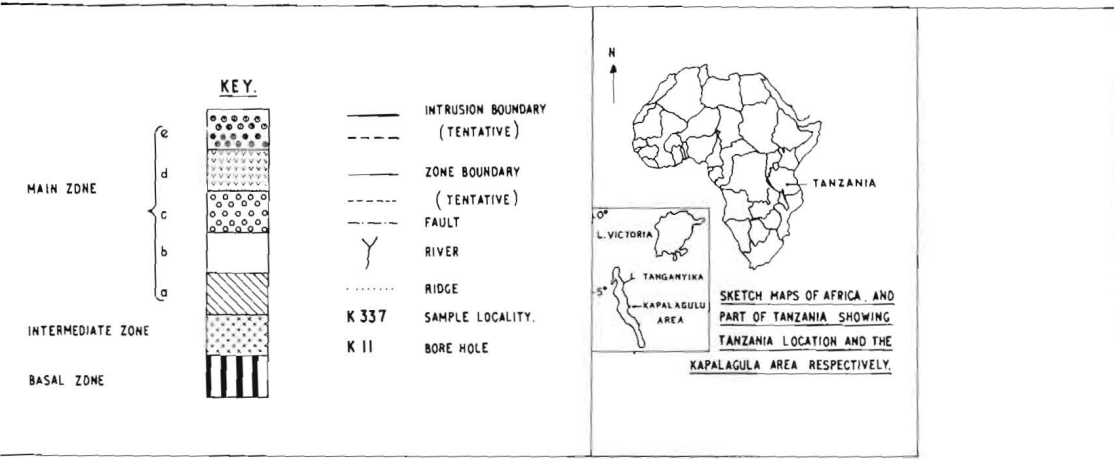
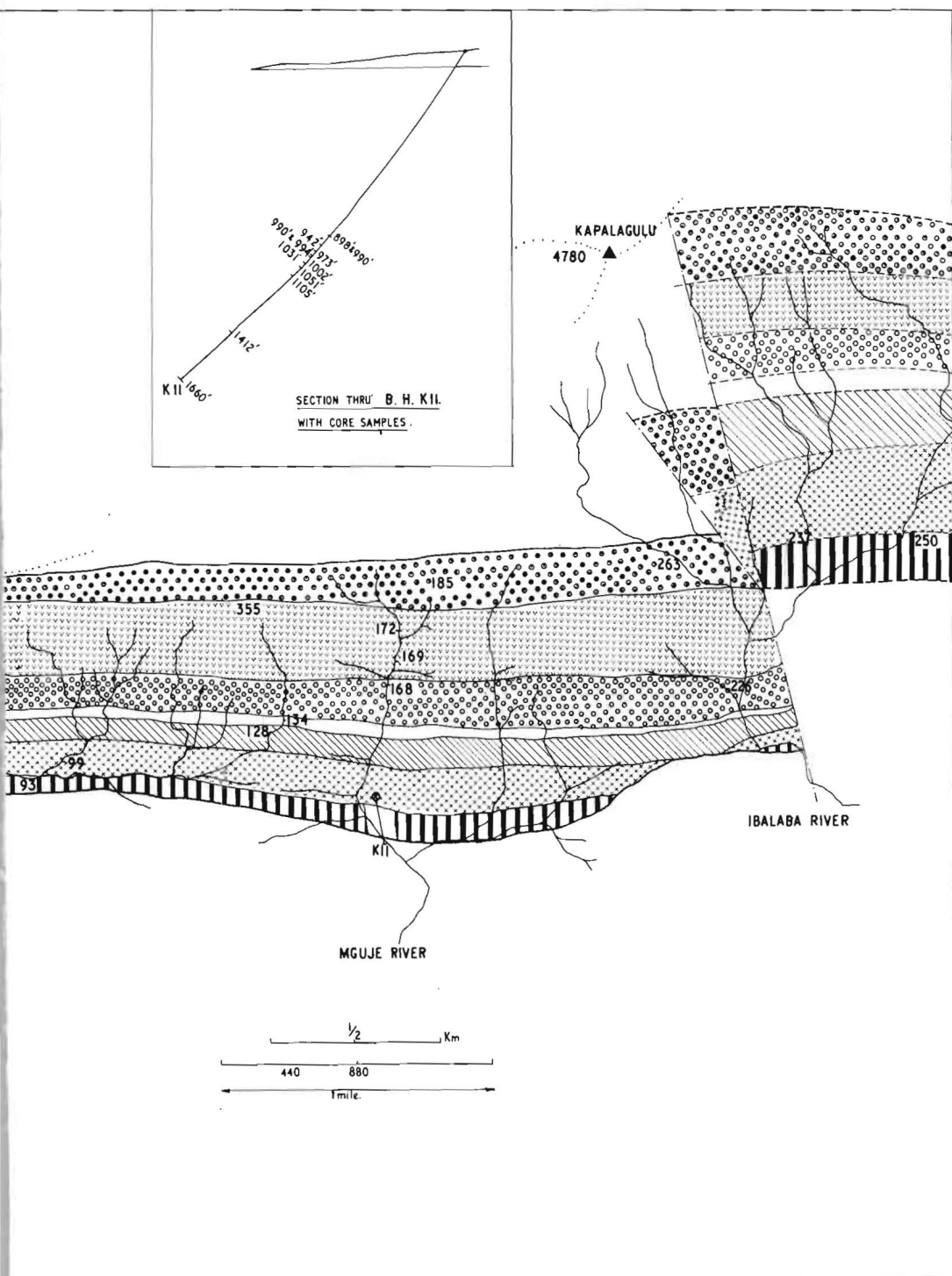


Fig. 1. Geological map of the Kapalagulu layered intrusion

Kapalagulu Intrusion, Tanzania.



showing sample localities (Tanzania, East Africa).

Table 2. Temperatures of Sub-Solidus Lamellae

Pyroxene Pair		Y(M1)	Y(M2)	PYX $_{aMg_2 Si_2O_6}$	Fe/Fe + Mg	Mg/Mg + Fe	T K	T ° C
K337	Opx Host	.965	.947	.379	.356	.644	1191.8	918.8
	Cpx Lam	.920	.141	.067	.279	.721		
K 70	Opx Lam	.957	.457	.200	.323	.677	1336.4	1063.4
	Cpx Host	.919	.201	.076	.357	.643		
K185	Opx Host	.875	.881	.190	.504	.496	1119.4	846.4
	Cpx Lam	.904	.165	.037	.503	.497		
K263	Opx Host	.957	.811	.199	.494	.506	1025	752.0
	Cpx Lam	.901	.191	.016	.417	.303		

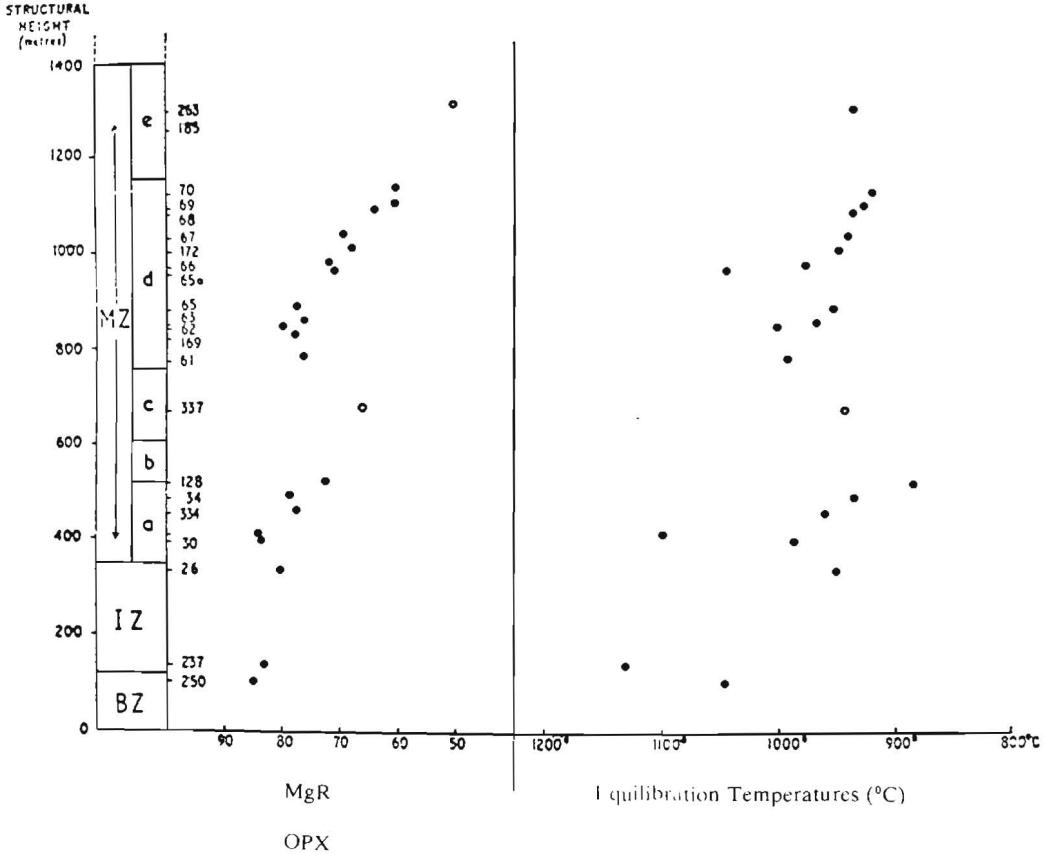


Fig. 3. Graphical representation of the variation of equilibration temperatures of coexisting Pyroxenes and the Cryptic variation in orthopyroxene with the structural height of Kapalagulu intrusion.

الترمومتر الجيولوجى للبيروكسينات فى معقد كابالاجولو المتطبق ، تنزانيا ، شرق افريقيا

أحمد عبدالقادر المهندس

قسم الجيولوجيا ، كلية العلوم ، جامعة الرياض ، المملكة العربية
السعودية •

يكون معقد كابالاجولو فى تنزانيا شرق إفريقيا تابعا طبقيًا من الصخور الفوق
القاعدية والقاعدية • وتتكون الصخور من المعادن الأساسية التالية :
الألوفين ، البلاجيوكليز ، والبايروكسين الغنى بالكالسيوم بالإضافة إلى
البايروكسين الفقير بالكالسيوم •

لقد استخدمت فى هذا البحث طريقة القياس الحرارى للبايروكسينات لدراسة
مراحل التبريد فى المعقد النارى بالإضافة إلى مقارنتها بالتغيرات الخفية التى
يبدىها معدن البيروكسين الفقير بالكالسيوم •

ويبدى البيروكسين الفقير بالكالسيوم تغيرا مرحليا حيث يتغير من
اورثوبايروكسين إلى بيجونيت مقلوب عند درجة حرارة (أقل من ١٠٠٠ م)
وهى أقل من درجة الحرارة التى يبدىها نفس المعدن فى معقد البشفيلد بأفريقيا
ولقد عينت أيضا درجات حرارة الاتزان لصفائح المحاليل المفلوطة فى البيجونيت
المقلوب •